AIP | Applied Physics Letters

Universal geometric classification of armchair honeycomb nanoribbons by their properties in a staggered sublattice potential

T. E. O'Brien, C. Zhang, and A. R. Wright

Citation: Applied Physics Letters **103**, 171608 (2013); doi: 10.1063/1.4827339
View online: http://dx.doi.org/10.1063/1.4827339
View Table of Contents: http://scitation.aip.org/content/aip/journal/apl/103/17?ver=pdfcov
Published by the AIP Publishing

Universal geometric classification of armchair honeycomb nanoribbons by their properties in a staggered sublattice potential

T. E. O'Brien,[1,2] C. Zhang,[2] and A. R. Wright[1,3,a)]
[1]*School of Mathematics and Physics, University of Queensland, Brisbane, 4072 Queensland, Australia*
[2]*School of Engineering Physics, University of Wollongong, New South Wales 2552, Australia*
[3]*Institute for Theoretical Physics, University of Leipzig, D-04103 Leipzig, Germany*

(Received 14 August 2013; accepted 15 October 2013; published online 25 October 2013)

We demonstrate the topological band-gap dependence of armchair honeycomb nanoribbons in a staggered sublattice potential. A scaling law is presented to quantify the band gap variation with potential strength. All armchair nanoribbons are described by one of three distinct classes depending on their width, consistent with previous classifications, namely, the well known massless Dirac condition, potentially gapless, and gapless-superlattice. The ability to tune and, in all cases close, the band-gap via external probes makes our classification particularly relevant experimentally. We propose several systems in which these results should shed considerable light, which have all already been experimentally realized. © *2013 AIP Publishing LLC*. [http://dx.doi.org/10.1063/1.4827339]

The search for states with topological origins is not a new one. The domain wall states in polyacetylene, commonly referred to as the Su-Schieffer-Heeger or SSH model,[1] and their field theoretic counterparts[2] as well as the TKNN invariant and the quantum Hall effect,[3] followed by the fractional quantum Hall effect and Chern-Simons theories,[4] are condensed matter examples which each span several decades. Undoubtedly, this ubiquitous field has recently enjoyed a renaissance due to the excitement surrounding topological insulators: time reversal invariant bulk insulators with a single gapless surface Dirac cone[5] and topological superconductors that may eventually support topological quantum qubits.[6]

The community's interest having been piqued; it is not surprising that graphene, the canonical example material with two-dimensional massless Dirac cones, not to mention the first material to have been considered as a topological insulator,[7] has been cut, bent, layered, crumpled, adsorbed, twisted, and stretched in order to demonstrate new and exotic topologically non-trivial states.[8–14] The overarching concept is quite simple: due to its two-sublattice (spinor) structure, winding numbers can be associated with the graphene Hamiltonian over the Brillouin zone.[14] By inducing a gap at the Dirac points then, the winding number can be engineered to be non-trivial, and thus edge states will arise. Even the flat bands in a zig-zag graphene nano-ribbon can be understood from this broad topological principle.[15] This has been a remarkably successful task, and graphene continues to produce new and unexpected physics.

It is well known that the low energy states in armchair graphene nanoribbons are, in general, massive. The two K points in bulk two dimensional graphene are projected onto each other in momentum space when the system is reduced to a quasi-one dimensional one, allowing the two massless cones to mix, thus producing a gap.[16] In the seminal paper by Brey and Fertig, this is easily seen by noting that the boundary conditions of the two sublattices must match in this special geometry.[17] In contrast, in the case of zig-zag ribbons only one sublattice constitutes each edge, thus preserving the gapless K point for all zig-zag edged ribbons. For this single crucial reason, zig-zag edged ribbons, samples, and interfaces are the usual candidate systems in which topologically borne states are proposed to exist.[18]

Here, we show that armchair edged ribbons with a staggered sublattice potential have a tuneable mass-gap which, in the case of gapped ribbons can be decreased, or even closed, by varying the potential strength and gradient. In complete analogy with the occurrence of massless Dirac ribbons, we show that with increasing width, *each effect is observed in every third ribbon*. We propose four realistic systems where these results may be observable: twisted bilayer graphene, chemically adsorbed single layer graphene, and lattice or substrate mismatched graphene and irradiated silicene. The geometric origin of the effects ensures their robustness, independent of ribbon width. This makes them particularly ideal for consistent practical applications. These geometric results follow from topological considerations, where the symmetry protected surface states[19] are broken by a symmetry-breaking mass gap, leading to a tuneable edge state structure for the ribbons.

In Figure 1 we show a typical ribbon that we are considering with the domain wall placed at a typical site i_W. The corresponding Hamiltonian which is the focus of the current work is $H = H_0 + V$, where H_0 is the tight-binding Hamiltonian of a honeycomb lattice which is given by

$$H_0 = \sum_{i}^{2W} \sum_{j}^{3} t_{ij} c^{\dagger}_{i+\hat{\delta}_j} c_i + \text{c.c.}, \tag{1}$$

where t_{ij} is the overlap integral of first nearest neighbouring sites $\langle i, j \rangle$, and is zero otherwise, and j denotes the three nearest neighbor vectors. In this formalism, the width of a ribbon or superlattice unit cell is $W\sqrt{3}|\hat{\delta}|/2$. To create a ribbon, we construct the appropriate unit cell and set $t = 0$ when a first

a)Electronic address: a.wright7@uq.edu.au

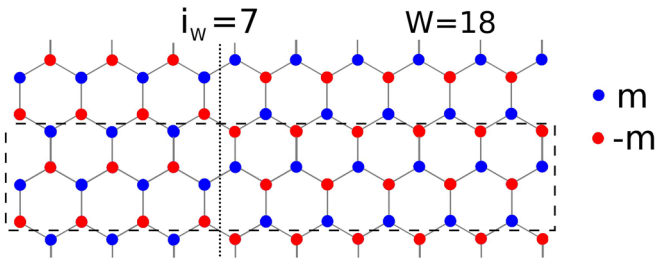

FIG. 1. A typical lattice structure (W/2 = 18, $i_W = 7$). At the domain wall, the position of the alternating positive (red) and negative (blue) sublattice potentials is changed from A+/B− to A−/B+, where A and B denote the index of individual pairs. The AB pairs are chosen so as to be positioned along the axis of the ribbon. The unit cell is shown by the dashed line.

nearest neighboring site leaves the edge of the ribbon, and to create a superlattice of ribbons with alternating sublattice potential, we adopt periodic boundary conditions instead. We also introduce a staggered sublattice potential across the width of the ribbon given by

$$V = \sum_{i}^{W/2} \mathrm{sgn}(i - i_W) m (c_i^\dagger c_i - c_{i+\hat{\delta}_1}^\dagger c_{i+\hat{\delta}_1}), \qquad (2)$$

where m is the magnitude of the potential and i_W marks the site in the unit cell where the potential changes sign, amounting to the location of a domain wall. Although this sharp change in sign is a specific choice, we stress that none of our results are qualitatively changed by a smooth change in sign of the potential, as is shown in Fig. 2. This reflects the topological nature of these states, namely, that the low energy

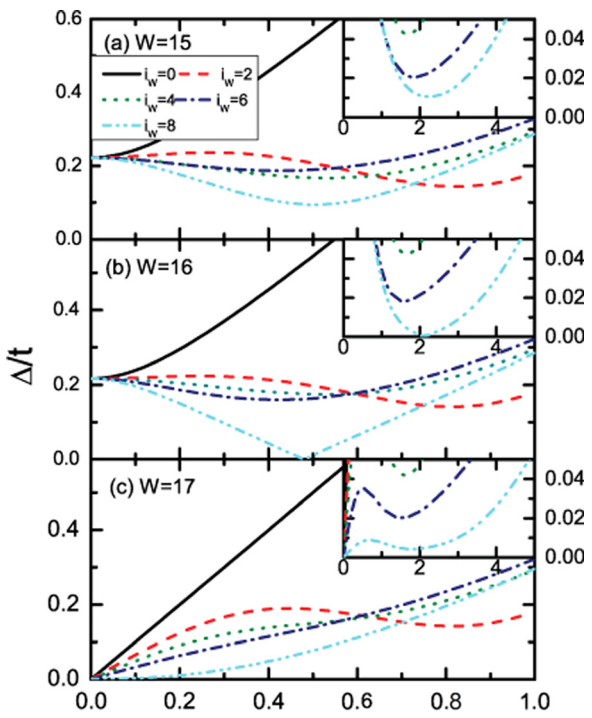

FIG. 2. Band gap trends with increasing m for (top to bottom) gapless superlattice, potentially gapless (with even number of A–B pairs), and Dirac ribbons. Note the large dip with all ribbons when $i_W = 2$, which is the smallest possible Dirac domain. Insets are for the same width of ribbon, but with a sinusoidally varying potential; we see that this does not alter the gap-closing condition, but instead decreases the integrated strength of the potential, and thus moves the gap-closing condition to larger values of m/t.

states are solitonic solutions in analogy with the SSH model, which, at particular, special points in paramater space do not hybridize, but in general do. Therefore, a smoothly varying potential merely increases the value of m at which the gap-closing condition is reached.

Upon diagonalising these systems, we first ask the following question: Is it possible to completely collapse the band gap of an armchair ribbon by applying a periodic potential? The answer to this question is yes, but only in one *sixth* of all possible ribbons, namely, those where $(W-4)/6 \in \mathbb{Z}$, and only when the $i_W = W/2$. We stress here that these ribbons are not Dirac ribbons ($(W-2)/3 \in \mathbb{Z}$). Ribbons where $(W-1)/6 \in \mathbb{Z}$ *almost* possess this quality; however, as they have an odd number of pairs in their unit cells, they cannot *strictly* fulfill the requirements of equally sized domains (W is odd, so $i_W = W/2 \pm 0.5$), even though the effect is identical. Therefore, these ribbons display extremely small minima of ϵ_{BG} compared with their non-Dirac counterparts ($W/3 \in \mathbb{Z}$). We label this class of armchair ribbons potentially gapless (PG), as a tuned staggered sublattice potential has the ability to tune the band-gap to zero, or nearly zero.

We now move on to the armchair superlattice. The system is now two-dimensional, and the lattice translation vectors are orthogonal. In general, the transverse component of the Hamiltonian is easily constructed as a two-site unit cell with lattice vectors trivially determined by i_W. The resulting bandstructure behavior along the transverse direction is cos-like. Due to the oscillating gap along the transverse direction, the band-gap position deviates from the Γ point. In particular, the direct band gap position moves between $k_x = 0$, $k_x = 2\pi/3$ and $k_x = \pi$, where π is the dimensionless edge of the Brillouin zone.

At the Γ point, Dirac and PG superlattices are gapped at $m = 0$; however, PG superlattices can close the gap at $m = \Delta$ as in the ribbon case. However, the third, so-far uncategorized, ribbon type here differs. This brings us to a definition for the third class of ribbons: those for which $W \in \mathbb{Z}$ are *always* gapless at the Γ point when $m = 0$. Thus, these superlattices are likened to armchair Dirac ribbons. This is a particularly important class of ribbon, as they show that a very weak modulation across a 2D sample can close the gap at the gamma point, thus destroying the valley degeneracy of a 2D sheet. (We should point out that this is strictly the low m limit, rather than $m = 0$, as the latter simply corresponds to an infinite honeycomb sheet with zone-folded energy bands.) This third class of "ribbon" we call gapless superlattice (GS) ribbons. The gap at the Γ point as a function of m is shown in Figure 3 by the solid black line. We have thus established that *all* honeycomb ribbons fall into one of the three classes of Dirac ($(W-2)/3 \in \mathbb{Z}$), potentially gapless ($(W-1)/3 \in \mathbb{Z}$), and gapless superlattice ($W/3 \in \mathbb{Z}$).

It is well known that armchair edged graphene nanoribbons fall into two distinct geometric classes, metallic and insulating.[20] The existing classification of armchair edged graphene nanoribbons with edge hydrogen passivation is also well known.[21] In this seminal work, the authors introduce a band-gap scaling law for the three types of graphene nanoribbon with edge hydrogen passivation. A tight-binding implementation of that model is one where the hopping integrals and on-site energies vary between the ribbon edges and

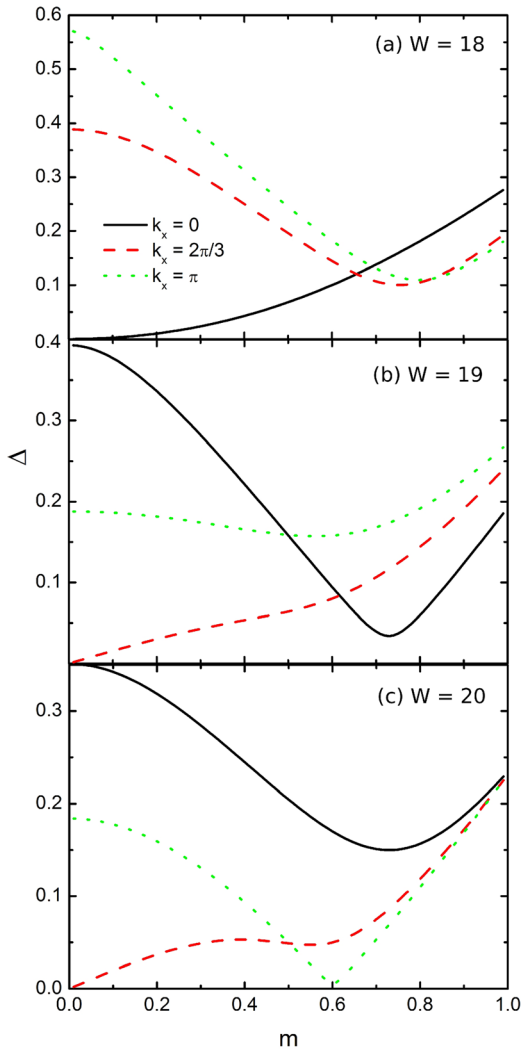

FIG. 3. The mass dependence of the band gap at the Γ point, $k_x = 2\pi/3$ and $k_x = \pi$. The behavior at the Γ point establishes the third universal classification of gapless superlattice "ribbons," which are the only armchair superlattices to become gapless as $m \to 0$. The other two points define the high-symmetry gapless points and band-inversion points, which are lifted for sufficiently large m. For each system, $i_W = 8$.

their bulk. The classification presented here shows that even the insulating phases can be tuned to become gapless, and differ markedly between themselves. Crucially, we suggest that all three types can be explored experimentally via appropriately tuned external fields. The different classifications are presented in Table. I.

The second important point in the superlattice Brillouin zone is $2\pi/3$, whose behavior with increasing m is shown in Figure 3 by the red dashed line. At this point, there is a band crossing between the top-most valence band and the lowest conduction band, leading to two Dirac points at $m = 0$ for Dirac and PG superlattices, directly corresponding to the two K points of a 2D sheet. As the mass increases, these bands can mix, and the Dirac points disappear. However, for some Dirac ribbons, the Dirac points move toward the Brillouin zone edge, and can fuse into one, before becoming massive, as can be seen in Fig. 3(c) by the green dotted line.

For the sake of experimental exploration of the parameter space in a controllable situation, we now briefly explore the relationship between the gradient of the gap as a function of m, i.e., $\partial\epsilon_{BG}/\partial m$ of Dirac ribbons, and the location of the domain wall, i_W. A quasi-linear scaling law is observed from numerical results, but ribbons where $i_W = 3n + 2$ and ribbons where $i_W = 3n + 3$ (with the same W) have the same gradient (for a given n). We find three scaling relationships here, one where the i_W is placed such that the smaller domain itself makes a PG ribbon, one where it makes a GS ribbon, and one where it makes a Dirac ribbon. The three scaling laws can be written compactly as

$$\left.\frac{\partial\epsilon_{BG}}{\partial m}\right\|_{m=0} = 1 - \frac{2i_W + i_W \mathrm{Mod}(3)}{W+1}, \tag{3}$$

which agrees within 0.05% to the computed values.

These results should prove useful in understanding the physics of several experimentally realized materials, particularly as the ability to produce samples with well defined edge termination becomes increasingly viable. The first is adsorbed graphene. Graphene has been successfully hydrogenated and fluorinated, which has produced some very interesting results.[22,23] However, a convincing physical model for either has thus far proven elusive. The results outlined in this work are particularly relevant to adsorbed graphene. It has been shown that randomly adsorbed graphene will tend toward uniform adsorption. In particular, in the case of semi-hydrogenated graphene, it has been shown that hydrogen atoms will tend to bond with just one of the two sublattices. However, it is extremely unlikely that randomly adsorbed graphene will become completely uniformly adsorbed, and instead should form domains.[24] Although the domain wall configuration presented here is ideal, the variation of the mass-gap as a function of domain wall position should prove useful for identifying the behaviour of different adsorbed samples. Further, via controlled substrate blocking, it is possible that the adsorption could be tunable in different samples. If possible, a two-gap system could be fabricated, even where the smaller gap could be vanishingly small.

TABLE I. The different classifications of armchair honeycomb nanoribbon band gaps Δ according to their widths W. δ is the variation in hopping near the edge of a hydrogen passivated ribbon, such that $t \to (1+\delta)t$. The new classification, presented here, is appropriate in staggered sublattice potentials, an experimentally relevant, and tuneable quantity, in particular, contexts.

$W/3 = p \in \mathcal{Z}$	$(W-1)/3 = p \in \mathcal{Z}$	$(W-2)/3 = p \in \mathcal{Z}$	Ref.
Insulating	Insulating	Metallic	20
$\delta\Delta \approx -\frac{8\delta t}{3p+1}\sin^2\frac{p\pi}{3p+1}$	$\delta\Delta \approx \frac{8\delta t}{3p+2}\sin^2\frac{(p+1)\pi}{3p+2}$	$\delta\Delta \approx \frac{2\lvert\delta\rvert t}{p+1}$	21
Gapless superlattice	Potentially gapless	Dirac	This work

Other systems of particular relevance to these results are twisted bilayer graphene and substrate or lattice-mismatched graphene.[25] The idea behind these systems is that bilayer graphene or graphene atop a substrate behaves as a single layer of graphene with a gauge field.[26] A twisted bilayer, for example, can be described as a single layer of graphene with an oscillating mass term (and gauge field which does not contribute to the gap). As the mass term changes sign, it forms a network of domain walls over the sample. It has been suggested that these domain walls *always* lie along an armchair edge.[16] Therefore, this system forms precisely the systems discussed above, where the magnitude of the mass depends on the interlayer spacing. Other forms of lattice-mismatched bilayer graphene as well as substrate mismatched graphene behave analogously.

Finally, silicene has recently emerged as an interesting graphene-like system with a buckled out-of-plane structure. Ezawa has pointed out that a simple Stark effect can be realised with an incident electric field which, due to the buckled lattice, realises a mass-gap precisely of the form considered here.[27] An inhomogeneous electric field, in this case, realises the very domain walls we have introduced.

In conclusion, we identified two geometric classes of armchair ribbon of period three in the width other than the usual Dirac class, namely, the potentially gapless class and the gapless-superlattice class. It is crucial for future experimental investigations, to understand that ribbons of *any* width can be made gapless and that bilayer systems, in particular, can be shown to have effective single layer behaviour that *necessarily* falls into one of these three classes. Finally, we proposed several systems that have already been realized experimentally to which these results are particularly relevant.

[1]W. P. Su, J. R. Schrieffer, and A. J. Heeger, Phys. Rev. B **22**, 2099 (1980).
[2]R. Jackiw and C. Rebbi, Phys. Rev. D **13**, 3398 (1976).
[3]D. J. Thouless, M. Kohmoto, M. P. Nightingale, and M. den Nijs, Phys. Rev. Lett. **49**, 405 (1982).
[4]S.-C. Zhang, T. H. Hansson, and S. Kivelson, Phys. Rev. Lett. **62**, 82 (1989).
[5]X.-L. Qi and S.-C. Zhang, Rev. Mod. Phys. **83**, 1057–1110 (2011).
[6]C. Nayak, S. H. Simon, A. Stern, M. Freedman, and S. Das Sarma, Rev. Mod. Phys. **80**, 1083 (2008).
[7]C. L. Kane and E. J. Mele, Phys. Rev. Lett. **95**, 146802 (2005).
[8]W. Yao, S. A. Yang, and Q. Niu, Phys. Rev. Lett. **102**, 096801 (2009).
[9]M. J. Schmidt and D. Loss, Phys. Rev. B **81**, 165439 (2010).
[10]R. Nandkishore and L. Levitov, Phys. Rev. B. **82**, 115124 (2010).
[11]I. Martin, Ya. M. Blater, and A. F. Morpurgo, Phys. Rev. Lett. **100**, 036804 (2008).
[12]J. Li, I. Martin, M. Buettiker, and A. F. Morpugo, Nat. Phys. **7**, 38 (2011).
[13]E. Rotenberg, Nat. Phys. **7**, 8 (2011).
[14]A. R. Wright, Sci. Rep. **3**, 2736 (2013).
[15]A. P. Schnyder and S. Ryu, Phys. Rev. B **84**, 060504(R) (2011).
[16]A. R. Wright and T. Hyart, App. Phys. Lett. **98**, 251902 (2011).
[17]L. Brey and H. A. Fertig, Phys. Rev. B **73**, 235411 (2006).
[18]G. W. Semenoff, V. Semenoff, and F. Zhou, Phys. Rev. Lett. **101**, 087204 (2008).
[19]X. Chen, Z.-X. Liu, and X.-G. Wen, Phys. Rev. B **84**, 235141 (2011).
[20]K. Nakada, M. Fujita, G. Dresselhaus, and M. S. Dresselhaus, Phys. Rev. B **54**, 17954 (1996).
[21]Y.-W. Son, M. L. Cohen, and S. G. Louie, Phys. Rev. Lett. **97**, 216803 (2006).
[22]D. C. Elias, R. R. Nair, T. M. G. Mohiuddin, S. V. Morozov, P. Blake, M. P. Halsall, A. C. Ferrari, D. W. Boukhvalov, M. I. Katsnelson, A. K. Geim, and K. S. Novoselov, Science **323**, 610 (2009).
[23]J. T. Robinson, J. S. Burgess, C. E. Junkermeier, S. C. Badescu, T. L. Reinecke, F. K. Perkins, M. K. Zalalutdniov, J. W. Baldwin, J. C. Culbertson, P. E. Sheehan, and E. S. Snow, Nano Lett. **10**, 3001 (2010).
[24]A. R. Wright, T. E. O'Brien, D. Beaven, and C. Zhang, App. Phys. Lett. **97**, 043104 (2010).
[25]A. Luican, G. Li, A. Reina, J. Kong, R. R. Nair, K. S. Novoselov, A. K. Geim, and E. Y. Andrei, Phys. Rev. Lett. **106**, 126802 (2011).
[26]M. Kindermann and P. N. First, Phys. Rev. B **83**, 045425 (2011).
[27]M. Ezawa, New J. Phys. **14**, 033003 (2012).